



CHORUS

This is the accepted manuscript made available via CHORUS. The article has been published as:

Revisited phase diagram on charge instability and lattice symmetry breaking in the organic ferroelectric TTF-QCl₄

Ryosuke Takehara, Keishi Sunami, Fumitatsu Iwase, Masayuki Hosoda, Kazuya Miyagawa, Tatsuya Miyamoto, Hiroshi Okamoto, and Kazushi Kanoda

Phys. Rev. B **98**, 054103 — Published 7 August 2018

DOI: [10.1103/PhysRevB.98.054103](https://doi.org/10.1103/PhysRevB.98.054103)

Separation of charge instability and lattice symmetry breaking in the organic ferroelectric, TTF-QCl₄; Phase diagram revisited

Ryosuke Takehara¹, Keishi Sunami¹, Fumitatsu Iwase^{1,*}, Masayuki Hosoda¹, Kazuya Miyagawa¹, Tatsuya Miyamoto², Hiroshi Okamoto^{2,3}, and Kazushi Kanoda^{1†}

¹ *Department of Applied Physics, University of Tokyo,
Bunkyo-ku, Tokyo, 113-8656, Japan*

² *Department of Advanced Materials Science,
University of Tokyo, Kashiwa, Chiba, 277-8561, Japan*

³ *AIST-UTokyo Advanced Operando-Measurement Technology
Open Innovation Laboratory (OPERANDO-OIL),
National Institute of Advanced Industrial Science
and Technology (AIST), Chiba 277-8568, Japan*

(Dated: July 5, 2018)

Abstract

There has been increasing interest in electronic ferroelectricity, which stems from deformation of the electronic wave function coupled with lattice symmetry breaking, invoking a Berry-phase description of electronic polarization beyond the conventional notion of ionic displacement. How does a ferroelectric transition of electronic nature cross over to a conventional one of ionic nature? This is a fundamental issue of ferroelectricity that is yet to be answered. Here, investigating a quasi-one-dimensional organic ferroelectric material, TTF-QCl₄, under pressures of up to 35 kbar, we reveal a pressure-temperature phase diagram, which spans the electronic and ionic regimes of ferroelectric transitions in a single material. The global phase diagram revealed by nuclear quadrupole resonance (NQR) experiments demonstrates that the electronic ferroelectricity crosses over to the conventional ionic ferroelectricity through the separation of the charge-transfer instability and the lattice symmetry breaking (dimerization) and that the previously reported dimer liquid phase is largely extended to high pressures.

PACS numbers: 76.60.Gv, 77.80.-e, 77.84.Jd

I. INTRODUCTION

The organic charge-transfer crystal TTF-QCl₄ (tetrathiafulvalene-*p*-chloranil), composed of one-dimensional alternating face-to-face stacks of donor (D) molecules, TTF, and acceptor (A) molecules, QCl₄ (Fig. 1a)¹, carries an emergent "electronic ferroelectricity" arising from an electronic displacement, which is distinguished from the conventional ionic displacement²⁻⁴. A key to understanding the novel ferroelectricity in TTF-QCl₄ is a neutral-to-ionic transition caused by a spontaneous charge transfer from TTF to QCl₄. It occurs when an increase of electronic occupation energy is surmounted by a gain of the Madelung energy in the ionic state under temperature or pressure variation⁵. At ambient pressure, TTF-QCl₄ is in a neutral state at room temperature but undergoes a charge-transfer transition to an ionic state at 81 K⁶, simultaneously accompanied by a lattice dimerization forming the donor-acceptor (DA) pairs⁷⁻⁹, which creates strongly charge-lattice-coupled ferroelectricity. The resultant polarization, which the classical framework fails to explain, is well described in terms of the electronic Berry phase^{3,4,10-13}.

Earlier experiments showed that the neutral-to-ionic transition occurs simultaneously with the dimerization transition (Fig. 1b) under pressures of up to ~ 6 kbar¹⁴⁻¹⁷; namely, it is the transition from neutral to ferroelectric ionic phases. Interestingly, it was also shown that a paraelectric ionic phase appears at higher pressures, separated from a ferroelectric ionic phase, although the pressure range studied was limited to below 9 kbar¹⁶. This implies that the polarization is less electronic in origin but more ionic, namely, more classical, under pressure. Thus, TTF-QCl₄ potentially serves as a platform for studying the link between the modern wave-like and classical particle-like pictures for ferroelectricity using pressure as a parameter. To clarify this missing link, we have extended the pressure study of this material up to 35 kbar by means of NQR, which is a microscopic probe of the charge/lattice state. As demonstrated by earlier experiments^{15,16}, charge transfer and lattice dimerization are directly signified by the profile of NQR lines, which appear at frequencies proportional to the electric-field gradient at the nuclear position, determined by the local charge distribution. Thus, we utilized the NQR probe to explore pressure-temperature phase diagram regarding charge transfer and lattice symmetry breaking.

II. EXPERIMENTAL

We performed ^{35}Cl NQR measurements on two polycrystalline samples of TTF-QCl₄, which contains four Cl atoms in QCl₄ (Fig. 1a), under zero magnetic field. The results for sample #1 and #2 are represented as open circles and triangles in Fig. 1b and 1c, respectively. NQR signals were acquired with the standard spin-echo techniques. Hydrostatic pressure, P , was applied to the sample using a BeCu/NiCrAl dual-structured clamp-type cell with Daphne 7373 ($P < 20$ kbar) and 7474 ($20 < P < 35$ kbar) oils as the pressure media. The solidification pressures of the Daphne 7373 and 7474 oils are approximately 22 and 37 kbar at room temperature, respectively, and thus, the hydrostaticity is maintained over the entire pressure range in this study. The pressure, which was maintained by clamping the pressure cell at room temperature, was somewhat reduced by solidification of the oils when the sample is cooled. This effect is corrected with reference to the reported calibration data¹⁸, in the pressure and temperature range where the effect is appreciable.

III. RESULTS AND DISCUSSION

A. NQR spectra and phase diagram

In the neutral phase of TTF-QCl₄, the crystal structure is monoclinic $P2_1/n^7$; the DADA arrangement is uniform (non-dimeric) and all the QCl₄ molecules are crystallographically equivalent. Each molecule has two inequivalent Cl atoms (labelled Cl1 and Cl2 in Fig. 1a) because an inversion centre is located on the QCl₄ molecule despite the absence of intramolecular mirror-reflection symmetry in the crystal. Thus, two NQR lines are observed in the neutral phase. At ambient pressure, we observed two ^{35}Cl NQR spectra at 37.54 and 36.96 MHz at 260 K, arising from the Cl1 and Cl2 sites. Both spectra behaved similarly; namely, their positions shifted to higher frequencies with decreasing temperature and split at $T_c \sim 82$ K, reproducing the previous NQR results^{19,20}. Thus, we investigated one of the two lines, residing on the higher frequency side.

Figure 2a shows the temperature evolution of a ^{35}Cl NQR line measured at ambient pressure (along arrow I in Fig. 1b). A single line in the neutral state at high temperatures splits into two lines when TTF-QCl₄ undergoes a ferroelectric transition at ~ 82 K because the two Cl atoms, Cl1 and Cl2, in QCl₄ become inequivalent due to inversion symmetry

breaking caused by DA dimerization⁷. The line splitting is accompanied by a clear shift of the centre-of-gravity of the lines, which signifies a change in molecular charge due to the neutral-to-ionic transition. The simultaneous line splitting and shift demonstrate that the charge transfer transition and the dimerization transition coincide, as earlier results indicated^{19,20}.

Next, we traced the NQR line under a pressure sweep of up to 35 kbar at room temperature (along arrow II in Fig. 1b). The NQR line shows a pronounced shift at ~ 9 kbar (Fig. 2b), which locates on the extrapolation of the ferroelectric transition line indicated by earlier reports¹⁵. This sharp line shift is attributable to the charge transfer as demonstrated by previous IR measurements²¹. Remarkably, however, no line splitting was observed; namely, the sharp charge transfer that occurs at ~ 9 kbar is not accompanied by the long-range order of lattice dimerization. Next, we fixed the pressure at 18.2 kbar and monitored NQR spectra on cooling from room temperature (along arrow III in Fig. 1b). A single line observed at room temperature splits below 258 K (Fig. 2c), accompanied by only a small spectral shift, indicating a dimerization transition with a vanishingly small charge transfer. These results suggest that the charge transfer and dimer order are decoupled at high temperatures and pressures.

To see the profiles of the charge transfer and the lattice instability in the P - T plane, we examined the temperature dependence of NQR spectra at pressures that were increased in small steps. The splitting of NQR frequency clearly identifies the dimerization transition for each pressure (Fig. 2d). The plot of the transition points in Fig. 1b reveals a novel P - T phase diagram in which the dimerization transition temperature unexpectedly ceases to increase with pressure at approximately 8 kbar and decreases at higher pressures.

B. Separation of charge transfer and dimerization transition

The molecular charge and inversion symmetry breaking in QCl_4 are probed by the centre-of-gravity frequency of the NQR line, ν_{Q} , and the line splitting, ν_{split} , respectively, whose temperature dependences are shown in Figs. 3a and 3b. It is also known that ν_{Q} varies with temperature in a generic manner due to the thermally activated molecular motion, which effectively reduces the anisotropy of the quadrupole tensor due to motional averaging^{22,23}. The pressure effect coming from the change of molecular packing can also change the electric-

field gradient. These effects on ν_Q can be separated from the effect of charge in question by treating the effect semi-empirically so that we can extract the degree of charge transfer, ρ , defined as $D^{+\rho}A^{-\rho}$ (Fig. 3c) from the ν_Q values (Fig. 3a) using the optical data in the following way^{21,24}.

First, we describe our analysis of the ν_Q data at ambient pressure. We make three assumptions: (i) at a given temperature, ν_Q depends linearly on ρ ; (ii) the proportionality coefficient A between the variations of ν_Q and ρ is independent of temperature; and (iii) the temperature dependence of ν_Q in the state of $\rho=0$, $\nu_Q=0$, obeys the empirical formula given by Koukoulas *et al.*, $\nu_Q^{\rho=0}(T) = \nu_0 \exp(-\alpha T^2)$, where ν_0 and α are constants²³. These assumptions are formulated as $\nu_Q(T) = A\rho(T) + \nu_0 \exp(-\alpha T^2)$. The value of A is estimated at -1.08 MHz/ ρ from the jump in NQR frequency at the ferroelectric transition, $\Delta\nu_Q(T_c) = 0.216$ MHz, and the change of ρ evaluated from the infrared spectroscopy measurements, $\Delta\rho^{\text{IR}}(T_c) = 0.20$ ²⁴. Then, we use the ν_Q and ρ^{IR} values at two temperatures, $T = 296$ K ($\nu_Q = 37.624$ MHz and $\rho^{\text{IR}} = 0.18$) and T_c^+ (the lowest temperature in the high-temperature phase, $\nu_Q = 37.888$ MHz and $\rho^{\text{IR}} = 0.33$)^{21,24} to determine the ν_0 and α values, which yields $\nu_0 = 38.296$ MHz and $\alpha = 2.02 \times 10^{-7}$ K⁻². Thus, the deduced relationship between ν_Q and ρ at ambient pressure is depicted in Fig. 4a.

Next, to extract the values under various pressures, we further assume that (iv) A , ν_0 , and α are independent of pressure and (v) the pressure effect is incorporated by adding a correction term, $\Delta\nu_Q(P)$, to the $\nu_Q(T)$ for any temperature. For $\Delta\nu_Q(P)$, we refer to the pressure dependence of the ³⁵Cl NQR frequency of the neutral QCl₄ crystal, $\nu_Q^{\text{QCl}_4}$, in which the degree of charge transfer is invariant under pressure variation. Figure 4b shows the pressure dependence of $\nu_Q^{\text{QCl}_4}$ at room temperature, which slightly increases with pressure up to 8 kbar and saturates at higher pressures. The pressure dependence, $\Delta\nu_Q^{\text{QCl}_4}(P) = \nu_Q^{\text{QCl}_4}(P) - \nu_Q^{\text{QCl}_4}(0)$, is fitted by the equation $\Delta\nu_Q^{\text{QCl}_4}(P) = a[1 - \exp(-bP)]$ with $a = 0.110$ MHz and $b = 0.379$ kbar⁻¹. Using this equation for the pressure effect, the relationship between ν_Q and ρ is eventually expressed as $\nu_Q(P, T) = A\rho(T) + \nu_0 \exp(-\alpha T^2) + a[1 - \exp(-bP)]$. Using this formula, we obtained the temperature dependence of ρ under various pressures as shown in Fig. 3c, which is qualitatively consistent with those of earlier optical measurements^{21,25-27}.

At ambient pressure, ρ is ~ 0.2 at room temperature and, on cooling, gradually increases to ~ 0.3 at 82 K, where it jumps above 0.5, coincidentally followed by the dimerization

transition. Under applied pressures, the jump in ρ , $\Delta\rho$, is diminished and nearly vanishes under ~ 7.5 kbar (Fig. 3d). At higher pressures, the ρ values are well above 0.5, indicating that the system is in the ionic state even before the dimerization transition, and these features of ρ are consistent with previous optical studies^{21,25-27}. At high pressures of 15 and 18.2 kbar, $\Delta\rho$ takes a slightly negative value (Fig. 3d), very probably because the largely transferred charge is backflowed by the molecular orbital hybridization between the DA pair promoted by the dimerization²⁸.

Figure 3e displays the variation of ρ with pressure at fixed temperatures. At 240 and 260 K, ρ shows sharp changes at pressures between 7.0 and 7.5 kbar, coinciding with the dimerization transition. Remarkably, even at 280, 300 and 320 K, when no dimer order was observed, ρ exhibits continuous but sharp changes in a narrow pressure range of 7.5 to 8.0 kbar. The contour plot of the ρ values in the P - T phase diagram (Fig. 1c) illustrates that the charge transfer and the dimer order, which coincide at low pressures, are separated above ~ 7.5 kbar. At ~ 8.5 -9 kbar, just above the bifurcation pressure, the line splitting, ν_{split} , on the transition to the dimer order nearly vanishes (Fig. 3b), indicating that the ferroelectric transition becomes second order around this pressure region. The change from the first-order to second-order transition imply the tricritical point that was suggested in a previous study¹⁶.

It was previously shown that small anomalies in NQR frequency, neutron diffraction intensity and broad maxima in dielectric permittivity signified the first-order charge transfer transition and the crossover, respectively, separated from the dimerization transition, which predicts the existence of a critical end point of the charge transfer¹⁵⁻¹⁷. On the other hand, at least in our experiments, as seen in the detailed temperature dependence of ρ (Fig. 3c), there was no discontinuous anomaly in ρ except for the dimerization transition at any pressure, indicating that the charge transfer occurs as a crossover.

C. Dimer liquid phase

The separation of the charge transfer and the lattice symmetry breaking means that an ionic phase without dimer order extends between the bifurcating lines (the red region in Fig. 1b). This result appears to be incompatible with an earlier study using infrared spectroscopy, which detected the molecular vibrational modes characteristic of DA dimerization

at pressures above 8 kbar^{27,29}, where the NQR experiments find no symmetry breaking. A key to a consistent understanding of the two seemingly inconsistent results is the time scale of the experimental probes. NQR detects the electronic and lattice states on a time scale of $\sim 10^{-7}$ s, whereas infrared spectroscopy captures their snapshot in the time domain of $\sim 10^{-12}$ s. If the DA dimers are not long-range ordered but fluctuating in between the two time scales, NQR spectra would yield a single line due to the motional narrowing whereas the infrared probe would detect the instantaneous dimerized states, which explains the two contrasting results coherently. We also remark on an X-ray-scattering anomaly observed at 11 kbar and 300 K³⁰, which was conjectured to indicate a ferroelectric transition and thus a continuous increase in ferroelectric transition temperature with pressure¹⁶. However, NQR lines are not split throughout the pressures studied at ambient temperature (Fig. 2b) and the temperature of symmetry breaking turns to a decrease above 8 kbar (Fig. 1c), indicating the extended paraelectric ionic phase in the P - T phase diagram. In this case, the X-ray-scattering anomaly, which in fact extends between 6.5 and 11 kbar³⁰, possibly reflects the variation of the charge transfer as shown in Fig. 5(a). The turnaround in the pressure evolution of the ferroelectric ordering temperature is consistent with the theoretical consequence that the energy gain of dimer formation shows a maximum and decreases with the increase of ρ ³¹; this is clearly illustrated in Fig. 3f, which shows the temperature of the dimer order against the value of ρ at the transition in the pressure range where ρ shows no or only a small jump upon the transition and lattice dimerization is the primary driving force of the transition.

A further indication of the dimer liquid state is given by the dynamical properties of NQR spectroscopy performed under fine pressure variation at room temperature (along line II in Fig. 1b). Figures 5a and 5b show the pressure evolutions of the degree of charge transfer and ³⁵Cl NQR relaxation rate $1/T_1$, respectively, which probes the fluctuations of the electric-field gradient arising from fluctuations of charge and/or lattice. At ~ 8 kbar, a charge transfer from TTF to QCl₄ occurs sharply (Fig. 5a), and concomitantly, $1/T_1$ increases (Fig. 5b), indicating that charge and/or lattice fluctuations are strongly enhanced in the transient pressure region of charge transfer. At higher pressures, the charge transfer is nearly complete (Fig. 5a); however, the $1/T_1$ values remain two orders of magnitude higher than in the neutral phase. This behaviour is similar to the pressure profile of ag-mode intensity in vibrational spectroscopy^{27,29}, suggesting that the large $1/T_1$ values even at

higher pressures than ~ 8 kbar is due to dimerization fluctuations in the charge-transferred ionic phase, consistent with the dimer liquid picture. Thus, the phase diagram of TTF-QCl₄ contains three distinct phases - a neutral phase, a paraelectric ionic phase and a ferroelectric ionic phase (Fig. 1b), in agreement with the previous results¹⁵⁻¹⁷, - which correspond to the gas, liquid and solid phases of dimers with respect to the lattice degrees of freedom; notably, the dimer liquid phase is extended in a wide pressure range. Three distinct phases are deduced from the quasi-one-dimensional spin-1 Blume-Emery-Griffiths (BEG) model that assigns spin ± 1 and spin 0 states to the dimerized ionic pair of $D^{+\rho}A^{-\rho}$ or $A^{-\rho}D^{+\rho}$ and the neutral pair of D^0A^0 (A^0D^0), respectively, where the paraelectric and ferroelectric ionic phases correspond to a condensate and crystal of charge-transfer segments, $D^{+\rho}A^{-\rho}$ or $A^{-\rho}D^{+\rho}$, respectively^{17,32}.

IV. CONCLUDING REMARKS

The ferroelectric order of TTF-QCl₄ at ambient and low pressures is of electronic origin²⁻⁴, which explains the large polarization observed in TTF-QCl₄, whereas the classical model of ionic displacement fails to explain it². At high pressures well above 8 kbar, the charge transfer is nearly complete, meaning that the ferroelectricity is classical. The phase diagram shown here (Fig. 1b) illustrates how the electronic ferroelectricity crosses over to the ionic one. When multiple degrees of freedom are involved in a phase transition, it is generally first order. The clear and simultaneous jumps in charge transfer and lattice dimerization is a manifestation of the strong coupling of charge and lattice, as expected in the regime of electronic ferroelectricity. As the pressure increases, however, the jumps are diminished, indicating that charge instability is decoupled from the lattice symmetry breaking at ~ 7.5 kbar (Fig. 3d). The separation of the charge transfer and dimer order is considered as an inevitable process that makes the electronic ferroelectricity cross over into the ionic one.

Electron transfer between different orbitals in adjacent molecules plays a primary role in the emergence of the electronic ferroelectricity of current interest, whereas the ionic displacement with electrons bound within respective molecules carries the conventional ferroelectricity. The present experiments reveal that, in an organic ferroelectric material, TTF-QCl₄, the former transitions to the latter through the separation of the charge transfer and lattice symmetry breaking. The separation of them possibly generates mobile neutral-ionic do-

main walls and solitons, which carry electric currents; indeed, recent theoretical studies^{33,34} suggested anomalous electric conductivity by such topological excitations.

Acknowledgments

We thank H. Fukuyama, M. Ogata and N. Nagaosa for critical discussions. This work was supported by the JSPS Grant-in-Aids for Scientific Research (S) (Grant No. 25220709) and for Scientific Research (C) (Grant No. 17K05846), and by CREST (Grant Number: JPMJCR1661), Japan Science and Technology Agency.

R.T., K.S., F.I., and M.H. contributed equally to this work.

* Current address: Department of Physics, Tokyo Medical University, Shinjuku-ku, Tokyo 160-8402, Japan

† Corresponding author, e-mail:kanoda@ap.t.u-tokyo.ac.jp

¹ J. J. Mayerle, J. B. Torrance, and J. I. Crowley, *Acta Crystallogr. Sect. B Struct. Crystallogr. Cryst. Chem.* **35**, 2988 (1979).

² K. Kobayashi, S. Horiuchi, R. Kumai, F. Kagawa, Y. Murakami, and Y. Tokura, *Phys. Rev. Lett.* **108**, 237601 (2012).

³ G. Giovannetti, S. Kumar, A. Stroppa, J. Van Den Brink, and S. Picozzi, *Phys. Rev. Lett.* **103**, 266401 (2009).

⁴ S. Ishibashi and K. Terakura, *J. Phys. Soc. Japan* **83**, 73702 (2014).

⁵ J. B. Torrance, J. E. Vazquez, J. J. Mayerle, and V. Y. Lee, *Phys. Rev. Lett.* **46**, 253 (1981).

⁶ J. B. Torrance, A. Girlando, J. J. Mayerle, J. I. Crowley, V. Y. Lee, P. Batail, and S. J. LaPlaca, *Phys. Rev. Lett.* **47**, 1747 (1981).

⁷ M. Le Cointe, M. H. Lemée-Cailleau, H. Cailleau, B. Toudic, L. Toupet, G. Heger, F. Moussa, P. Schweiss, K. H. Kraft, and N. Karl, *Phys. Rev. B* **51**, 3374 (1995).

⁸ A. Girlando, F. Marzola, C. Pecile, and J. B. Torrance, *J. Chem. Phys.* **79**, 1075 (1983).

⁹ Y. Tokura, Y. Kaneko, H. Okamoto, S. Tanuma, T. Koda, T. Mitani, and G. Saito, *Mol. Cryst. Liq. Cryst.* **125**, 71 (1985).

- ¹⁰ R. Resta and D. Vanderbilt, in *Phys. Ferroelectr. A Mod. Perspect.*, edited by K. M. Rabe, C. H. Ahn, and J.-M. Triscone (Springer, 2007), pp. 31-68.
- ¹¹ R. D. King-Smith and D. Vanderbilt, *Phys. Rev. B* **47**, 1651 (1993).
- ¹² D. Vanderbilt and R. D. King-Smith, *Phys. Rev. B* **48**, 4442 (1993).
- ¹³ R. Resta, *Rev. Mod. Phys.* **66**, 899 (1994).
- ¹⁴ K. Takaoka, Y. Kaneko, H. Okamoto, Y. Tokura, T. Koda, T. Mitani, and G. Saito, *Phys. Rev. B* **36**, 3884 (1987).
- ¹⁵ M. Lemée-Cailleau, M. Le Cointe, H. Cailleau, T. Luty, F. Moussa, J. Roos, D. Brinkmann, B. Toudic, C. Ayache, and N. Karl, *Phys. Rev. Lett.* **79**, 1690 (1997).
- ¹⁶ M. Buron-Le Cointe, E. Collet, B. Toudic, P. Czarnecki, and H. Cailleau, *Crystals* **7**, 285 (2017).
- ¹⁷ T. Luty, H. Cailleau, S. Koshihara, E. Collet, M. Takesada, M. H. Lemée-Cailleau, M. B.-L. Cointe, N. Nagaosa, Y. Tokura, E. Zienkiewicz, and B. Ouladdiaf, *Europhys. Lett.* **59**, 619 (2002).
- ¹⁸ K. Murata, H. Yoshino, H. O. Yadav, Y. Honda, and N. Shirakawa, *Rev. Sci. Instrum.* **68**, 2490 (1997).
- ¹⁹ M. Gourdji, L. Guibé, A. Péneau, J. Gallier, B. Toudic, and H. Cailleau, *Solid State Commun.* **77**, 609 (1991).
- ²⁰ J. Gallier, B. Toudic, Y. Delugeard, H. Cailleau, M. Gourdji, A. Peneau, and L. Guibe, *Phys. Rev. B* **47**, 688 (1993).
- ²¹ H. Matsuzaki, H. Takamatsu, H. Kishida, and H. Okamoto, *J. Phys. Soc. Japan* **74**, 2925 (2005).
- ²² H. Bayer, *Zeitschrift Für Phys.* **130**, 227 (1951).
- ²³ A. A. Koukoulas and M. A. Whitehead, *Chem. Phys. Lett.* **167**, 379 (1990).
- ²⁴ S. Horiuchi, Y. Okimoto, R. Kumai, and Y. Tokura, *J. Phys. Soc. Japan* **69**, 1302 (2000).
- ²⁵ A. Dengl, R. Beyer, T. Peterseim, T. Ivek, G. Untereiner, and M. Dressel, *J. Chem. Phys.* **140**, 244511 (2014).
- ²⁶ M. Dressel and T. Peterseim, *Crystals* **7**, 17 (2017).
- ²⁷ M. Masino, A. Girlando, and A. Brillante, *Phys. Rev. B* **76**, 64114 (2007); M. Masino, N. Castagnetti, and A. Girlando, *Crystals* **7**, 108 (2017).
- ²⁸ N. Nagaosa, *J. Phys. Soc. Japan* **55**, 2754 (1986).
- ²⁹ H. Okamoto, T. Koda, Y. Tokura, T. Mitani, and G. Saito, *Phys. Rev. B* **39**, 10693 (1989).
- ³⁰ R. M. Metzger and J. B. Torrance, *J. Am. Chem. Soc.* **107**, 117 (1985).

- ³¹ A. Painelli and A. Girlando, Phys. Rev. B **37**, 5748 (1988).
- ³² J. Kishine, T. Luty, and K. Yonemitsu, Phys. Rev. B **69**, 75115 (2004).
- ³³ H. Fukuyama, and M. Ogata, J. Phys. Soc. Japan **85**, 23702 (2016).
- ³⁴ M. Tsuchiizu, H. Yoshioka, and H. Seo J. Phys. Soc. Japan **85**, 104705 (2016).

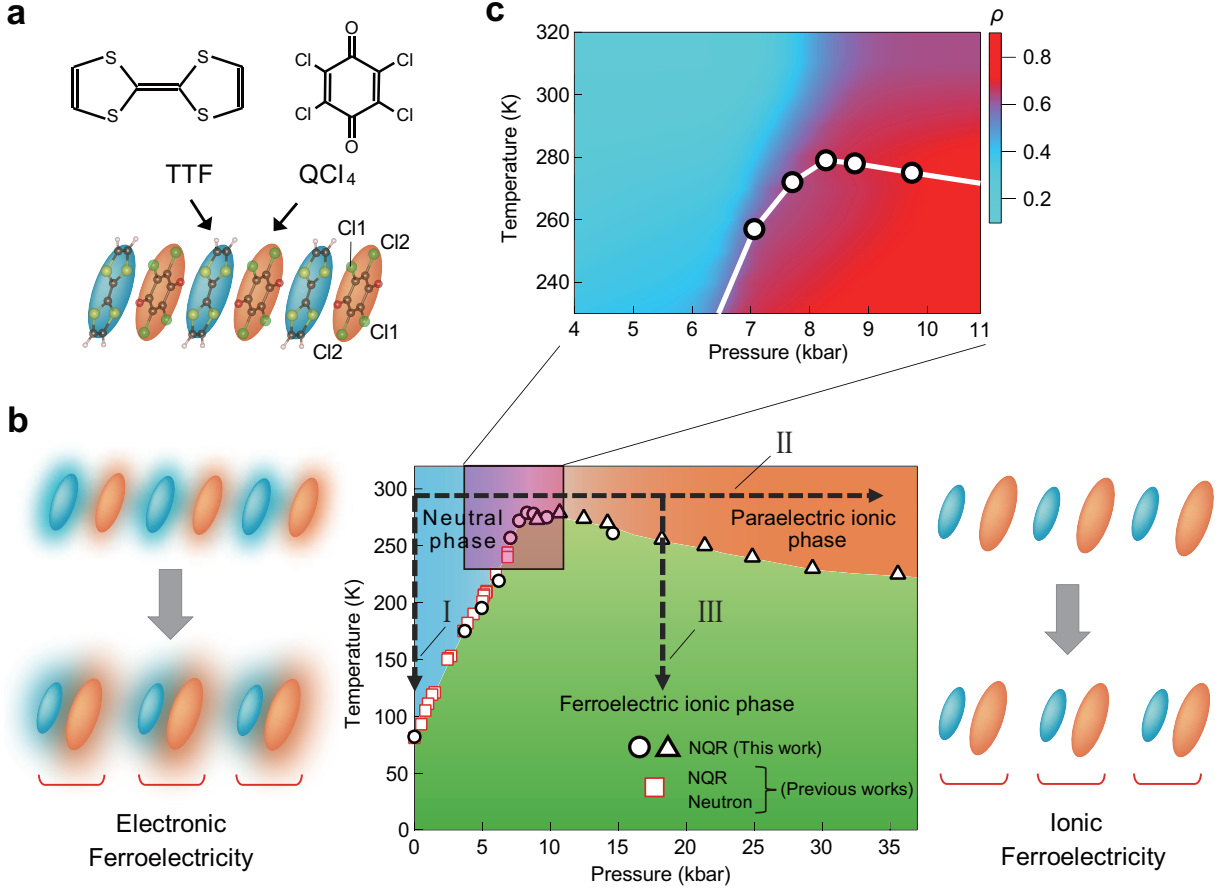


FIG. 1: (Color online) Structure and pressure-temperature phase diagram of TTF-QCl₄. **a**, One-dimensional alternating stack of TTF and QCl₄ molecules in the neutral state. **b**, Pressure-temperature phase diagram of TTF-QCl₄ determined by NQR experiments (black open circles and black triangles); the former is obtained from sample #1 studied under fine pressure control, whereas the latter is from sample #2 studied in a wide pressure range up to 35 kbar. Red open squares indicate previous results obtained from NQR and neutron experiments¹⁵. The ferroelectricity is dominated by the modification of the electronic wave at low pressures (left figure), whereas it is caused by an ionic displacement at high pressures (right figure). The size of the ellipsoid schematically expresses the total electron density in the HOMO (highest occupied molecular orbital) and LUMO (lowest unoccupied molecular orbital). **c**, Profile of the degree of charge transfer, ρ , defined as $\text{TTF}^{+\rho}\text{QCl}_4^{-\rho}$, in the squared region of the P - T phase diagram in **b**. The data of sample #1 studied under fine pressure tuning are used.

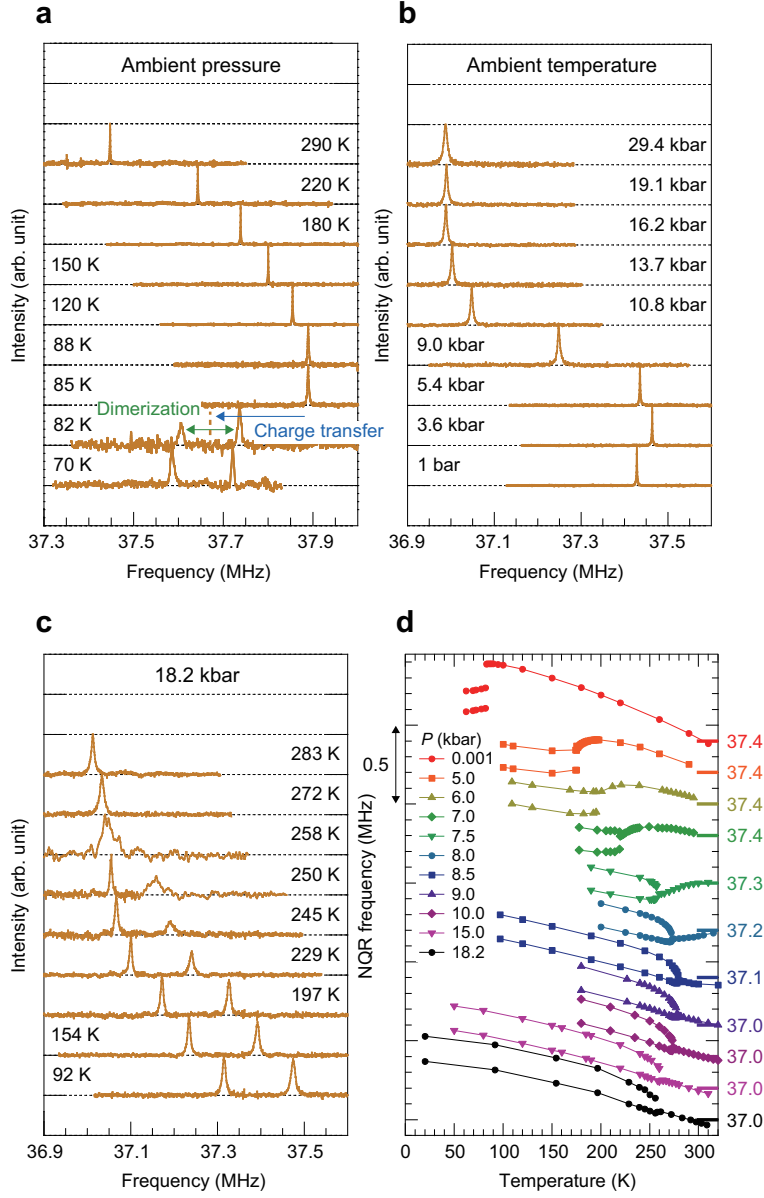


FIG. 2: (Color online) NQR spectra and pressure-temperature profile of NQR frequency. **a-c**, ^{35}Cl NQR spectra measured under temperature variation at ambient pressure (**a**), under pressure variation at ambient temperature (**b**), and under temperature variation at 18.2 kbar (**c**). The broken line in the 82 K spectrum in **a** represents the position of the centre-of-gravity of the spectrum. The line splitting to a doublet in **a** and **c** indicates the dimerization transition, which causes a lattice symmetry breaking. The abrupt shift in the centre-of-gravity of the spectrum signifies a charge transfer. **d**, NQR frequencies plotted against temperature for fixed pressures. The vertical scale (NQR frequency) is offset for each value of pressure for clarity; the reference values of frequency for each pressure are indicated on the right axis with the tick marks. The pressure values labelled in the panel are the room-temperature values.

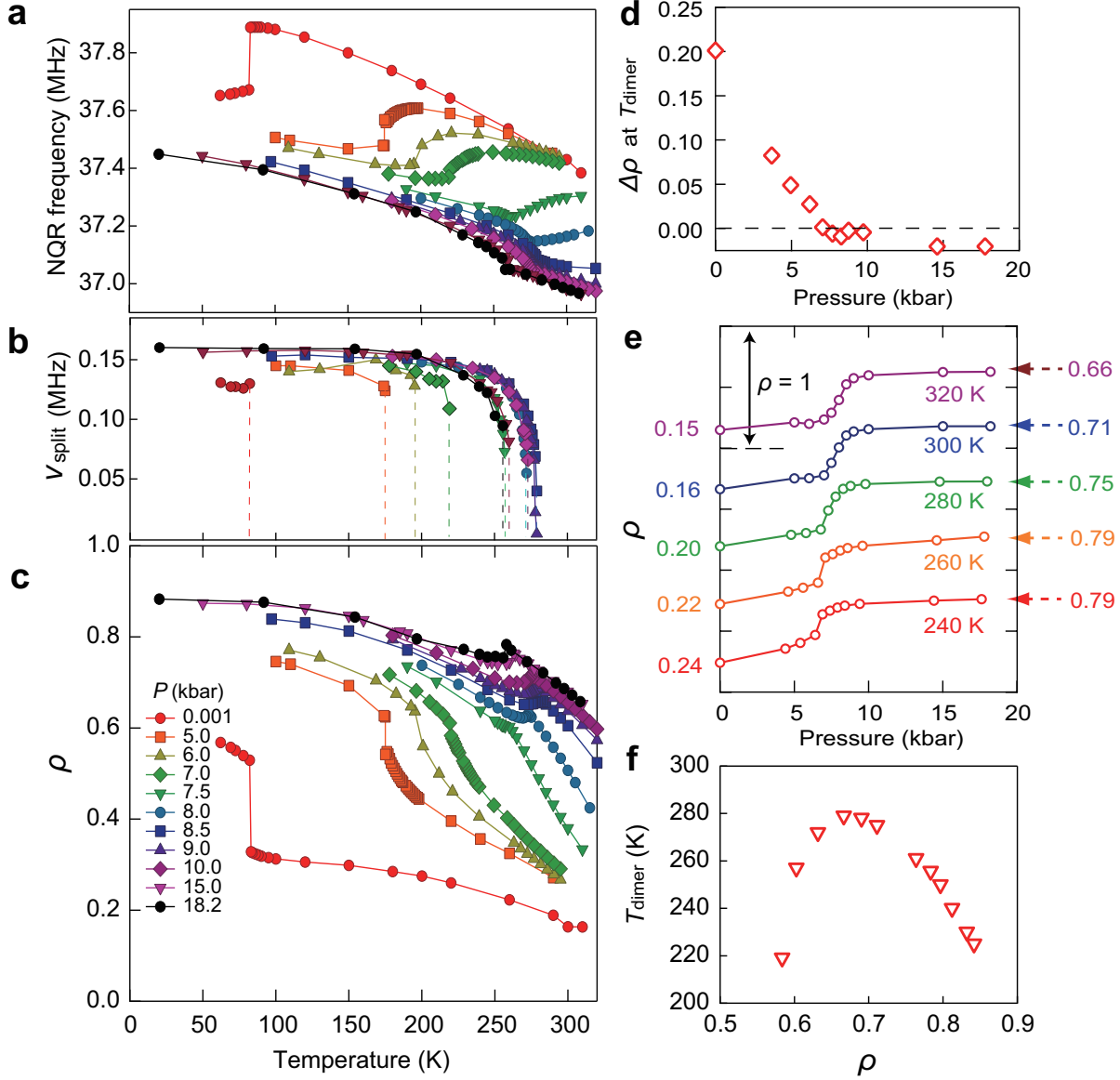


FIG. 3: (Color online) Degree of charge transfer and lattice dimerization. **a-c**, Temperature dependences of NQR frequency ν_Q (**a**), NQR line splitting ν_{split} (**b**), the degree of charge transfer, ρ , (**c**), under various pressures. The magnitude of ν_{split} is a measure of the degree of dimerization. The value of ρ is deduced from the value of ν_Q . The pressure values labelled in the panel are the room-temperature values. **d**, Discontinuity in ρ at the dimerization transition, $\Delta\rho$, for each pressure. **e**, The degree of charge transfer, ρ , plotted against pressure at fixed temperatures indicated in the panel. The data for 320 K are extrapolated values at each pressure. The pressure values of the horizontal axes in **d** and **e** are ones corrected for the temperature dependence of pressure. **f**, Dimerization transition temperature plotted as a function of the ρ value at the transition above 7.0 kbar, where ρ shows no appreciable jump upon transition.

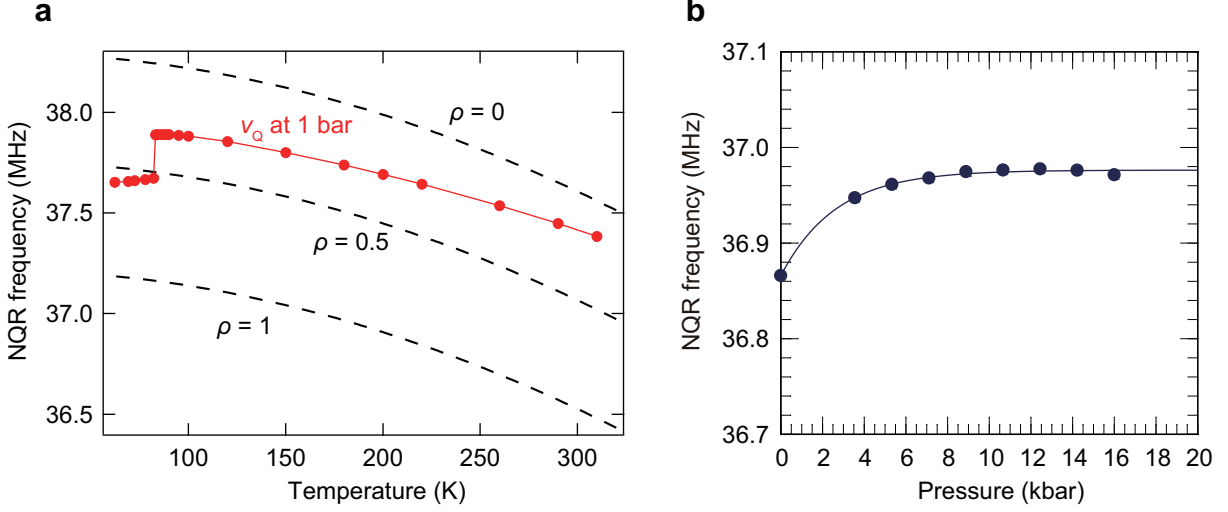


FIG. 4: (Color online) Relationship between ^{35}Cl NQR frequency and the degree of charge transfer ρ . **a**, Temperature dependence of ^{35}Cl NQR frequency. The red points indicate the experimental ν_Q data at 1 bar; the red line is a guide for the eye. The broken lines represent the calculated temperature dependences of NQR frequency for $\rho = 0$ (upper), 0.5 (middle) and 1 (lower). **b**, Pressure dependence of ^{35}Cl NQR frequency in neutral QCl_4 crystals. The line is a fit of the form $a[1 - \exp(-bP)]$ to the experimental data of $\Delta\nu_Q^{\text{QCl}_4}(P) = \nu_Q^{\text{QCl}_4}(P) - \nu_Q^{\text{QCl}_4}(0)$, which yields $a = 0.110$ MHz and $b = 0.379$ kbar $^{-1}$.

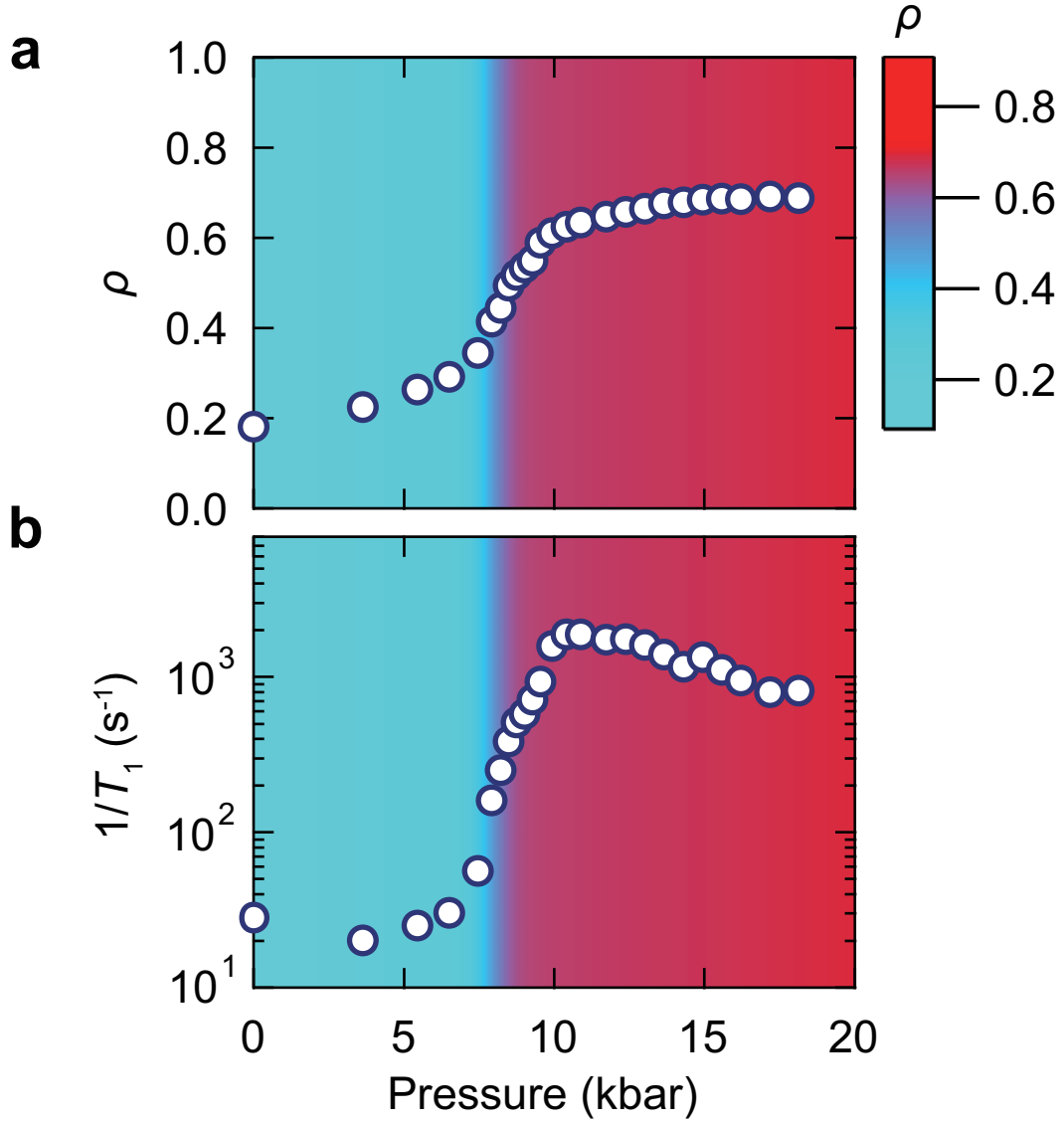


FIG. 5: (Color online) Variation of the degree of charge transfer, NQR relaxation rate on crossover from a neutral state to an ionic dimer-liquid state. **a**, Pressure dependence of the degree of charge transfer ρ (**a**), ^{35}Cl NQR spin-lattice relaxation rate $1/T_1$ (**b**) at room temperature. The ρ values in **b** are estimated from the NQR frequency ν_Q . The range of colour in **a** and **b** corresponds to the value of ρ as in Fig. 1c.